PROCEEDINGS A

royalsocietypublishing.org/journal/rspa

Perspective

Cite this article: Scholes GD. 2023 A molecular perspective on quantum information. *Proc. R. Soc. A* **479**: 20230599. https://doi.org/10.1098/rspa.2023.0599

Received: 17 August 2023
Accepted: 12 October 2023

Subject Areas:
chemical physics, physical chemistry

Keywords:
exciton, coherence, entanglement, quantum science

Author for correspondence:
Gregory D. Scholes
e-mail: gscholes@princeton.edu

A molecular perspective on quantum information

Gregory D. Scholes

Department of Chemistry, Princeton University, Princeton, NJ 08544, USA

GDS, 0000-0003-3336-7960

Some of the fundamentals of quantum information science are described, including the concepts of quantum resources, quantum states and mixedness of states. The explanations are detailed and include a combination of basic facts with fully worked examples, and some more advanced topics. The principles of quantum information are illustrated with chemical examples drawn from singlet fission, photophysics of radicals, molecular excitons, electron transfer and so on. Suggestions for prospects and challenges for the field are discussed.

1. Introduction

Quantum information science has become especially prominent in the past decade. Emerging from fundamental developments in our understanding of the quantum world, applications of quantum science are poised to change technologies. Concomitantly, researchers across a breadth of fields are interested in seeking new phenomena that are explained by quantum mechanics. However, a challenge is that the concepts at the core of quantum science can be difficult to appreciate properly. Even entanglement, an iconic property unique to quantum systems, has subtle and sometimes technical implications. Entanglement can be defined relatively easily, but a first understanding tends to open more questions than it answers.

Owing, in part, to the development of ultrafast laser experiments that can prepare superpositions and resolve the evolution of superposition states known as wavepackets, researchers have been interested in coherence phenomena in molecular and biological systems [1]. The field opens many fundamental questions and issues such as identifying function that arises from underlying non-classical dynamics. More recently still,

THE ROYAL SOCIETY PUBLISHING

there has been interest in working out how chemical systems will be useful for quantum information science and related technologies [2]. To identify opportunities more lucidly, it is important to appreciate fundamentally what constitutes quantum resources. It is also an open challenge to describe and identify quantum correlations in complex molecular systems. Ways of addressing these kinds of problems might be inspired by a physical understanding of the basis of quantum information.

The goal of the present paper is to give an introductory review of concepts in quantum information science, illustrated by examples relevant to chemical systems. The paper is not a review of progress, nor is it a complete technical exposition. Instead, the goal is to explain the basics with sufficient transparency and physical intuition. Examples of chemical systems are provided to give context to the intersection of molecular science and quantum information.

More detailed accounts of quantum information can be found in various books and reviews [3–8]. In a complementary paper [9] we describe the idea of entanglement and qubits, develop the concept of a general quantum state and touch on the main ideas behind quantum information itself. In that work, we made an effort to explain what are quantum correlations and how they differ from classical correlations.

2. Challenges for chemical quantum science

The following challenges motivate the content of this paper:

(a) How can we use entanglement as a resource in complex molecular systems? Entanglement is a powerful quantum correlation, but it is likely limited to relatively short length scales in real chemical systems. How can we use it to direct chemical transformations or photophysics?
(b) How can we use coherence as a resource? There is interesting potential for long-range coherence based on molecular aggregates or polaritons. Can coherence be exploited to enable new sensors or to control ultrafast dynamics by correlating remote molecular components? Such correlations might enhance quantum interference, providing a means of constructing quantum coherent circuits at the molecular scale [10].
(c) Measuring quantum correlations in complex systems remains a challenge, even if we were to know details of the relevant quantum state. Can experiments be devised that reveal evidence for non-classical correlations?
(d) Localized or separated unpaired electron spins in molecules can be harnessed to promote chemical reactions. Can entanglement of these spins be used to enable 'quantum-concerted' reactivity? Can a two-step reaction be more specifically guided to a product using techniques like teleportation that can direct a sequence of spin correlations among electrons?

3. Entanglement as a resource

If we are going to develop chemical systems that are relevant for quantum science, technology or metrology, we need first to articulate: What is a resource for quantum information science? A framework for devising how to exploit quantum states to enable processes or function is laid out by quantum resource theories [11]. The ingredients of a quantum resource theory are free states, free operations and resources. Examples of free states are separable states or incoherent states—generally states that are readily available. Similarly, free operations are easily implementable. They map free states to free states. The crucial ingredients are the resources. Resources include entangled states and coherent states. In the following sections we show examples of how entanglement can be exploited as a resource.

In the following, we often refer to canonical pure states of two entangled qubits, labelled A and B, often called the Bell states. We consider each qubit a two-state system, so that qubit A, for example, can be in state $|0\rangle_A$ or $|1\rangle_A$. In terms of these basis states for each of the two qubits, we

can write out the Bell states:

$$|\Psi_+\rangle = \frac{1}{\sqrt{2}}\Big[|0\rangle_A|1\rangle_B + |1\rangle_A|0\rangle_B\Big] \tag{3.1}$$

$$|\Psi_-\rangle = \frac{1}{\sqrt{2}}\Big[|0\rangle_A|1\rangle_B - |1\rangle_A|0\rangle_B\Big] \tag{3.2}$$

$$|\Phi_+\rangle = \frac{1}{\sqrt{2}}\Big[|0\rangle_A|0\rangle_B + |1\rangle_A|1\rangle_B\Big] \tag{3.3}$$

and

$$|\Phi_-\rangle = \frac{1}{\sqrt{2}}\Big[|0\rangle_A|0\rangle_B - |1\rangle_A|1\rangle_B\Big]. \tag{3.4}$$

(a) Superdense coding

The following example is taken from Nielsen & Chuang [3]. It illustrates how a quantum resource (entanglement) can help one party, Alice, to transmit two classical bits of information over a long distance to a second party, Bob. By exploiting the properties of qubits, Alice can send these two classical bits (00, 10, 01 or 11) using a single qubit, a protocol known as superdense coding.

A sketch of the procedure is as follows. To start, two qubits are entangled to produce $|\Phi_+\rangle$. Alice is given qubit A, while Bob takes qubit B. Alice can now perform a quantum operation (see below) on her qubit in isolation. She will then send the resulting (single) qubit to Bob. Bob, once in possession of both qubits, performs a measurement on the entangled pair to read out which Bell state is encoded. Using a predefined 'look-up' table, Bob associates whichever Bell state he holds with a pair of classical bits. For instance:

$$\Psi_+ \to 00$$

$$\Psi_- \to 01$$

$$\Phi_+ \to 10$$

and

$$\Phi_- \to 11.$$

Notice that two qubits are needed to encode two classical bits, we have the same total information supplied by four Bell states as four classical pair states. But, by making use of entanglement, Alice can communicate any pair of classical bits by *sending* only one qubit.

To be more explicit about the quantum operation employed by Alice, we can make use of the representation of quantum states and operators on the complex matrices. Recall that the initial entangled state comprising both qubits is

$$|\Phi_+\rangle = \frac{1}{\sqrt{2}}\Big[|0\rangle_A|0\rangle_B + |1\rangle_A|1\rangle_B\Big]. \tag{3.5}$$

Alice is given the qubit labelled A:

$$|\phi_A\rangle = |0\rangle_A + |1\rangle_A \tag{3.6}$$

that we can represent as the complex-valued vector

$$M_A = \begin{bmatrix} 0 \\ 1 \end{bmatrix}. \tag{3.7}$$

An operator on M_A takes the form of a 2×2 matrix that multiples M_A, thus mapping it to another vector in this (two-dimensional complex) Hilbert space. Specifically, Alice uses maps known as 'quantum gates'. Here is how it works.

To send 00 to Bob, Alice simply applies the identity gate, then the original entangled state ends up in Bob's possession. To send 10, Alice applies the quantum NOT gate, X to her qubit:

$$X\phi_A = \begin{bmatrix} 0 & 1 \\ 1 & 0 \end{bmatrix}\begin{bmatrix} 0 \\ 1 \end{bmatrix} = \begin{bmatrix} 1 \\ 0 \end{bmatrix}. \tag{3.8}$$

When Bob collects both qubits, he finds he holds $|\Psi_+\rangle$, which corresponds to 10 in the look-up table. To send 01, Alice applies the quantum phase-flip gate, Z to her qubit:

$$Z\phi_A = \begin{bmatrix} 1 & 0 \\ 0 & -1 \end{bmatrix} \begin{bmatrix} 0 \\ 1 \end{bmatrix} = \begin{bmatrix} 0 \\ -1 \end{bmatrix}, \tag{3.9}$$

thus providing Bob with Φ_-, which corresponds to 01 in the look-up table. To send 11, Alice applies the sequence of gates ZX (equivalent to iY, where Y is the Pauli-Y gate) to her qubit. Bob will then acquire $|\Psi_-\rangle$. When checking the working, remember that states that differ by an overall phase are equivalent, so $|\Psi_-\rangle$ and $|-\Psi_-\rangle$ denote the same state.

(b) Quantum teleportation

Teleportation allows a party, Alice, to transfer a quantum state $|\psi\rangle_a$ to a remote party, Bob, by operating locally on a shared entangled state. The final read-out by Bob of the teleported qubit is enabled by Alice sending Bob two classical bits. Here is a summary of the idea, with some detail, using an example taken from Barnett [6].

Alice and Bob share the state

$$|\Psi_-\rangle_{AB} = \frac{1}{\sqrt{2}}\Big[|0\rangle_A|1\rangle_B - |1\rangle_A|0\rangle_B\Big], \tag{3.10}$$

which serves as the 'quantum channel'. Alice wants to transfer to Bob the state $|\psi\rangle_a = \alpha|0\rangle_a + \beta|1\rangle_a$. To do that, Alice prepares the three-qubit state:

$$|\psi\rangle_a \otimes |\Psi_-\rangle_{AB} = \Big[\alpha|0\rangle_a + \beta|1\rangle_a\Big]\frac{1}{\sqrt{2}}\Big[|0\rangle_A|1\rangle_B - |1\rangle_A|0\rangle_B\Big]. \tag{3.11}$$

Alice's first step is to measure her two qubits in the Bell state basis of those bits. Let us rewrite equation (3.11) in that basis:

$$\begin{aligned} |\psi\rangle_a \otimes |\Psi_-\rangle_{AB} = \frac{1}{2}\Big[&|\Psi_-\rangle_{aA}\big(-\alpha|0\rangle_B - \beta|1\rangle_B\big) + |\Psi_+\rangle_{aA}\big(-\alpha|0\rangle_B + \beta|1\rangle_B\big) \\ &+ |\Phi_-\rangle_{aA}\big(\alpha|1\rangle_B + \beta|0\rangle_B\big) + |\Phi_+\rangle_{aA}\big(\alpha|1\rangle_B - \beta|0\rangle_B\big)\Big]. \end{aligned} \tag{3.12}$$

Clearly, because Alice's measurement projects onto one of the four basis states (here the Bell states), there are four equally probable outcomes of Alice's measurement, $|\Psi_-\rangle_{aA}$, $|\Psi_+\rangle_{aA}$, $|\Phi_-\rangle_{aA}$ or $|\Phi_+\rangle_{aA}$. Each of these possibilities leaves Bob holding a qubit in one of four distinct states, $(-\alpha|0\rangle_B - \beta|1\rangle_B)$, etc. The key is that each of those latter states can be converted to Alice's original qubit $|\psi\rangle_a$ by the action of one of a set of four operators (the Pauli operators). Alice uses her two classical bits to tell Bob which operator to apply. Bob performs the operation and now holds a qubit identical to Alice's original $|\psi\rangle_a$. Thus, the idea of teleportation is that a sequence of operations overlapping on a shared qubit can appear to transmit 'instantaneously' a state.

Wasielewski and co-workers have reported an example of 'hard-wired' teleportation of a spin state by photo-induced electron transfer in a supramolecular system [12]. The hard-wiring refers to the fact that Alice does not get to tell Bob which Pauli operator to apply, so he defaults to the unit operation. The qubits are spin states located on molecular fragments and the overall system comprises three connected molecular fragments, figure 1. The sequence of operations is shown in the figure. Notice that the order of these operations is a little different than the idealized example described above.

Alice holds her special qubit that is prepared by the experimenter (the radical). Optical excitation prepares the entangled state shared by Alice and Bob; the singlet excited state produces a singlet charge-transfer state by the photo-induced electron transfer reaction. Now, Alice returns to the ground state by transferring her electron to the radical molecule—however, because the radical was prepared in a specified spin state to start with, Alice must collapse the singlet charge-transfer state in such a way that her transferred electron spin pairs with the radical species. This,

(*a*) Alice prepares her qubit using a magnetic field and a microwave pulse

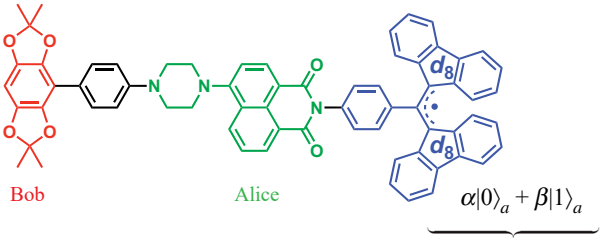

A spin doublet state is prepared with orientation relative to an applied magnetic field: Alice wants to share this state with Bob.

(*b*) Photo-induced charge separation entangles Alice and Bob

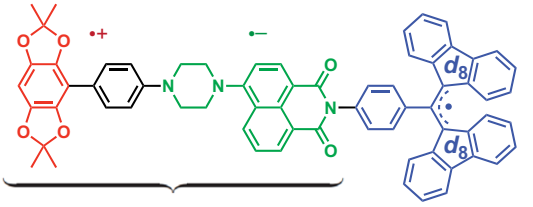

The green chromophore is photo-excited to a singlet state, then spontaneous charge separation produces a singlet state shared between the red and green chromophores.

(*c*) Electron transfer from Alice to her qubit teleports the qubit state

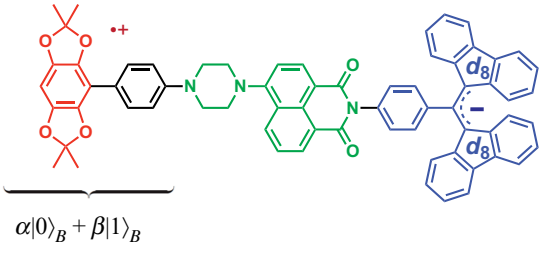

Charge transfer from the green to the blue molecule leaves Bob holding a double state radical, identical to Alice's original qubit.

Figure 1. (*a–c*) Schematic flow of the operations that teleport a qubit from the right side of the supramolecular complex to the left side. Adapted from Rugg *et al*. [12].

in turn, leaves Bob holding a qubit (the doublet hole state) that is identical to the qubit that was previously hosted by Alice's radical.

This is a good example of how molecular systems can demonstrate quantum operations. We see an intuitive physical manifestation of a quantum phenomenon masked as well-studied supramolecular photophysics. The process that turns a pair of sequential electron transfer reactions into teleportation is the set-up of the initial state of the unpaired electron on the molecule labelled R. The teleported state was read out, and thus characterized, using electron paramagnetic resonance (EPR) spectroscopy. The example shows how radical states will likely be important for chemical quantum information.

The molecular system also serves an example of how to think about the distance range for practical teleportation using chemical systems. The range will be limited by decoherence of the

entangled spins, which becomes difficult to preserve as the molecular fragments get further apart. That general concept is discussed in a later section.

4. Quantum states

Chemistry focuses on states, which are especially prominent in spectroscopy. We know that the better resolved a set of states is in a spectrum, then the quantum mechanical origin and properties of those states are more obvious. For example, when detailed electronic, vibrational and even rotational levels of a molecule are resolved in specialized gas phase spectroscopies, then the quantum mechanical description of the molecule is required to quantitatively and incisively explain the spectrum. Whereas, in solution at ambient temperature, the electronic absorption spectrum of a solute chromophore is sufficiently broadened by stochastic solute-solvent interactions that the quantum mechanical levels are mixed and obscured. As a consequence, the spectrum can be modelled reasonably well using a classical correlation function, and we find that interchromophore quantum mechanical states and dynamics are unlikely to be observed.

These well-known examples show that quantum states display clear and robust quantum properties when their eigenvalues are well resolved in the spectrum of all the states being measured in the spectral window of interest. Here we explain some pedagogical examples to provide insight and intuition for how ensemble averaging can diminish the quantum mechanical nature of a state.

(a) Averaging obscures phase

We perform measurements by projecting a state onto our measuring apparatus. The measurement is the average over a sequence of outcomes. In the case of a classical system, our ensemble yields properties of the probability distribution with respect to an appropriate random variable. For example, the distribution of energy states of a gas gives the probability that a molecule chosen at random will have a kinetic energy within a certain energy interval.

The challenge for measurements on quantum systems is to construct an analogous map from the set of states to a probability distribution [13] such that we account for the phase encoded in superpositions. These states are given by the density matrix ρ, or density operator [14,15]. The idea of ρ is that it provides expectation values of all bounded operators on the relevant Hilbert space—that is, the results of measurements on our ensemble of quantum systems. This works because the eigenvalues of ρ reflect the probability distribution of the states.

The density matrix comprises an average, at the amplitude level, over the distribution of states that are measured. A key consequence of that average is that quantum correlations disappear unless the phases of each state in the distribution are more-or-less in lock-step. We can get a sense of that by considering an explicit example.

The density matrix for a system with a finite number of basis states can be constructed as follows. We average over a sequence of N measurements, where each measurement gives us a state $|\Psi_j\rangle$ for system j in the ensemble:

$$\rho = \sum_{j=1}^{N} p_j |\Psi_j\rangle\langle\Psi_j|, \tag{4.1}$$

where p_j is the probability of measuring $|\Psi_j\rangle$. The density matrix is written in terms of the expansion of $|\Psi_j\rangle$ in the chosen basis

$$|\Psi_j\rangle = c_{1j}\psi_1 + c_{2j}\psi_2 + \cdots, \tag{4.2}$$

where c_{mj} are complex coefficients. Then, assuming our measurement solely resolves states j (e.g. the lowest energy eigenstate or those that carry the oscillator strength), the mn entry of the density

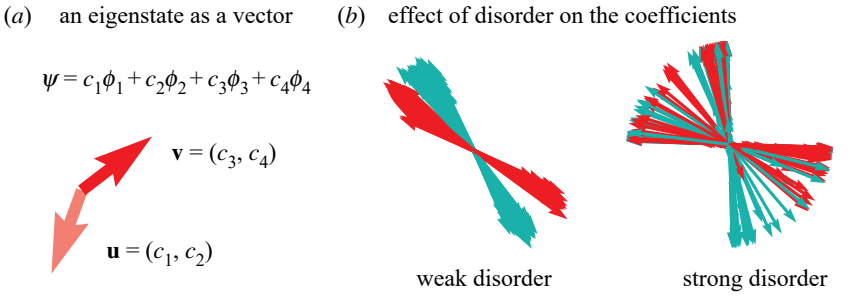

Figure 2. (*a*) Coefficients were calculated for a 4 × 4 Hamiltonian matrix with off-diagonal couplings according to the nearest-neighbour coupling model. Random off-sets to the four site energies were added for each copy of the system before each matrix is diagonalized. The phase of each eigenstate is represented by a double vector that shows direction, not magnitude, of the coefficient. (*b*) An ensemble of eigenstates generated with different ratios of electronic couplings to standard deviation of the distribution of diagonal disorder. Notice that the coefficients fan out in the phase space (constrained by symmetry of the eigenstate) as disorder dominates over electronic coupling.

matrix is

$$\rho_{mn} = \sum_{j=1}^{N} p_j c_{mj} c_{nj}^{*}. \tag{4.3}$$

Equation (4.3) shows how we can calculate the density matrix in practice. Considering each eigenstate $|\Psi_j\rangle$ in our ensemble in turn, we construct its contribution to the density matrix, multiply by the probability p_j and add that to the accumulating ensemble average. If we consider N eigenstates selected at random from the ensemble, then every $p_j = 1/N$. Sometimes our measurement might probe a specific energy window or interval, so then we only include in our average those eigenstates whose eigenvalues lie in that window.

The off-diagonal values in the density matrix (written in an appropriate basis) indicate how well the eigenstate phases are correlated within the ensemble. An example is shown in figure 2, discussed in more detail in Scholes [16]. Here we consider the single-excitation subspace (not the complete tensor product space) of four interacting qubits. Further, we focus on the lowest-energy eigenstate only. The coefficients were calculated for the lowest-energy eigenstate of a 4 × 4 Hamiltonian matrix with nearest-neighbour off-diagonal electronic couplings [17]. Random off-sets to the four site energies were added for each copy of the system before each matrix was diagonalized. In figure 2, we show a diagram that depicts the distribution of lowest-energy eigenstates in the ensemble by plotting the four coefficients as a pair of vectors, **u** and **v**. Notice how **u** equates the first two coefficients of the eigenstate as (x, y) coordinates, while **v** does that for the last two coefficients. Thus, in figure 2*b*, we can see how the wavefunction coefficients for the eigenstate corresponding to the lowest energy eigenvalue in an ensemble of wavefunctions become more loosely locked in phase as the disorder in the frequency of each site becomes larger—the coefficient vectors fan out because their relative phases lose correlation from one matrix to the next.

When the phases of the eigenvector coefficients are entirely uncorrelated from one member of the ensemble to the next, then the off-diagonal part of the density matrix is zero, and the state is said to be a perfectly mixed state—there is no coherence in this basis. For example, by inspecting equation (4.3) we can see that if the relative phases of basis states in each $|\Psi_j\rangle$ in the ensemble are random, so that in the case of real coefficients, $c_{mj}c_{nj}^{*}$ are sometimes positive, sometimes negative, then the off-diagonal values of ρ vanish once we take the average. You can compute that easily if you write out the concrete example of the density matrix for a 50–50 mixture of the two Bell states $|\Psi_+\rangle$ and $|\Psi_-\rangle$. The lack of quantum correlations in a perfectly mixed state is independent of the basis chosen to define ρ or the measurement. When ρ is diagonal, its eigenvalues correspond to the classical probabilities of a measurement returning an expectation value for each of the basis

states. That is the case because ρ has unit trace (the sum of its diagonal elements equals 1) and it is positive semi-definite.

Now, with a sense for what constitutes a quantum state, we can discuss entanglement and how it differs from classical correlation. The way we usually think about quantum correlations is by gauging how far from a fully mixed state is the state of interest [18]. That is, we can compare mixedness of a state, which we will address later in the paper. A deeper issue is that it is difficult to pinpoint a general state as being entangled. Not being able to detect whether or not an arbitrary state is entangled is a problem, because we are looking for states with the property of entanglement. As a starting point, instead we define an entangled state as a state that is 'not separable'.

(b) Separable states

A state is separable in the Hilbert space comprising the tensor product of the Hilbert spaces of the subsystems A and B, $\mathcal{H} = \mathcal{H}_A \otimes \mathcal{H}_B$ if it can be written [19,20]

$$\rho = \sum_{i=1}^{N} p_i \rho_i^A \otimes \rho_i^B. \tag{4.4}$$

If two subsystems, A and B, are entangled, then we cannot construct the composite state using only what we know about the subsystems separately, unlike separable states. This is because the superpositions of product states introduce non-additive correlations into the quantum probability distribution that are encoded in the density matrix of the composite system, but hidden to measurements performed on each subsystem separately.

The concept of separable versus non-separable states is explained by some examples. The general procedure we will use in the examples is as follows. Consider two arbitrary qubits, ψ_A and ψ_B. Let us say we know the density matrix ρ for the composite system. How can we find out if A and B are separable or entangled? Our approach is to see if ρ satisfies equation (4.4), in which case it is separable. To do that, we perform a sequence of measurements on the qubit A, and find its density matrix to be

$$\rho_A = \begin{bmatrix} c_A & d_A \\ d'_A & c'_A \end{bmatrix}, \tag{4.5}$$

where c_A, etc., are values in the real or complex field. We see from ρ_A that ψ_A is sometimes in the state $|0\rangle_A$, sometimes in $|1\rangle_A$ and sometimes in the superposition of those states. We do the same for B, to find

$$\rho_B = \begin{bmatrix} c_B & d_B \\ d'_B & c'_B \end{bmatrix}. \tag{4.6}$$

Now evaluate $\rho_A \otimes \rho_B$, noting that the result has the form of a matrix of matrices, thus giving the result

$$\rho_A \otimes \rho_B = \begin{bmatrix} c_A c_B & c_A d_B & d_A c_B & d_A d_B \\ c_A d'_B & c_A c'_B & d_A d'_B & d_A c'_B \\ d'_A c_B & d'_A d_B & c'_A c_B & c'_A d_B \\ d'_A d'_B & d'_A c'_B & c'_A d'_B & c'_A c'_B \end{bmatrix}. \tag{4.7}$$

In our purely academic setting we can ask, does this predicted density matrix match the ρ we measured for the composite system? If so, then the qubits are separable.

The first example is very simple. We perform a sequence of measurements on the product state of our composite system comprising the qubits A and B. We find that 25% of the time we measure $|0\rangle_A|0\rangle_B$, 25% of the time we measure $|1\rangle_A|0\rangle_B$, 25% of the time we measure $|0\rangle_A|1\rangle_B$ and 25% of

the time we measure $|1\rangle_A|1\rangle_B$. The density matrix is diagonal, with values of $\rho_{ii} = 1/4$. We write it with rows and columns indexed as $|0\rangle_A|0\rangle_B$, $|0\rangle_A|1\rangle_B$, $|1\rangle_A|0\rangle_B$, $|1\rangle_A|1\rangle_B$:

$$\rho_{AB} = \rho_A \otimes \rho_B = \begin{bmatrix} \frac{1}{4} & 0 & 0 & 0 \\ 0 & \frac{1}{4} & 0 & 0 \\ 0 & 0 & \frac{1}{4} & 0 \\ 0 & 0 & 0 & \frac{1}{4} \end{bmatrix}. \tag{4.8}$$

This is a fully mixed (classical) state which, of course, is separable.

It is not so straightforward to display more general examples. Peres [19] devised a clever technique to write a guaranteed mixed state, and this provides a good model for us. Consider a pure singlet state ($|\Psi_-\rangle$). This singlet state will make up a fraction x of our mixed state, while the remaining $(1 - x)$ fraction is a 'random fraction', comprising an equal admixture of the singlet and three triplet states to produce a fully mixed fraction of the state. The random fraction contributes a value of $(1 - x)/4$ to each diagonal element of ρ_{mixed}:

$$\rho_{\text{mixed}} = \begin{bmatrix} \frac{(1-x)}{4} & 0 & 0 & 0 \\ 0 & \frac{(1+x)}{4} & -\frac{x}{2} & 0 \\ 0 & -\frac{x}{2} & \frac{(1+x)}{4} & 0 \\ 0 & 0 & 0 & \frac{(1-x)}{4} \end{bmatrix}. \tag{4.9}$$

If we consider ρ_{mixed} with $x = 0$, then the state is fully mixed, by design, and the density matrix is diagonal, like the previous example. If $x = 1$ the state should not be separable. Indeed, there is obviously no way to write it as prescribed by equation (4.7) because we would require either $c_A = 0$ or $c_B = 0$ to set the first (top left) diagonal element to zero. But that contradicts that fact that the middle two diagonal elements are both non-zero. It is known [19], see appendix A, that this state is separable only if $x < \frac{1}{3}$, defining a cross-over between these extreme cases of separability and non-separability.

(c) Classical correlations

To start, let us write out the density matrix for the product state of our two qubits, A and B in the Hilbert space $\mathcal{H}_{\mathcal{AB}} = \mathcal{H}_A \otimes \mathcal{H}_B$, using the same basis as above, assuming no correlations at all. In other words, we find the subsystem A to be in the state $|0\rangle_A$ with probability p_A and the state $|1\rangle_A$ with probability $q_A = 1 - p_A$, similarly for B. Further, joint measurements find no correlations between the state of A and B. Thus, the resulting separable, fully mixed state is

$$\rho_{AB} = \rho_A \otimes \rho_B = \begin{bmatrix} p_A p_B & 0 & 0 & 0 \\ 0 & p_A q_B & 0 & 0 \\ 0 & 0 & q_A p_B & 0 \\ 0 & 0 & 0 & q_A q_B \end{bmatrix}. \tag{4.10}$$

Now let us add a strong classical correlation, whereby if we measure qubit A to be in the state $|0\rangle_A$, then qubit B is certain to be in the state $|1\rangle_B$, whereas if qubit A is found to be in the state $|1\rangle_A$, then qubit B is certain to be in the state $|0\rangle_B$. Despite the strong correlation between the measured outcomes on A and B—similar to outcomes of related measurements on the Bell states—the density matrix remains separable, and completely mixed. All that changes is that $p_A = q_B$ and $q_A = p_B$, so that

$$\rho_{AB} = \rho_A \otimes \rho_B = \begin{bmatrix} 0 & 0 & 0 & 0 \\ 0 & p_A^2 & 0 & 0 \\ 0 & 0 & p_B^2 & 0 \\ 0 & 0 & 0 & 0 \end{bmatrix}. \tag{4.11}$$

Thus, as anticipated above, the quantum correlations, like entanglement, defy explanation by classical correlations. Moreover, it is clear now how the quantum correlations come hand-in-hand

with classical-like correlations. That is, classical correlations like those evidenced in equation (4.11) are present, together with quantum correlations, in equation (4.9) with $x = 1$. Physically, this is the same idea as interference, like seen in the double slit experiment. First-order interference is insufficient evidence for uniquely quantum correlations, even though it demonstrates wave-like properties.

There are many examples of classical correlations exhibited by chemical systems. These include synchronization produced by feedback loops, oscillating reactions, or any switched system under kinetic control. Although these are interesting phenomena, they are not directly relevant for quantum information science.

(d) Mixedness of quantum states

It is sometimes helpful to compare how mixed one state is compared with another. As a basic introduction to this idea, here we examine a quantity known as purity, computed as $\mathrm{Tr}\,\rho^2$.

We have explained in Wu & Scholes [9] that the set of density matrices is a convex set, where the pure states are the extreme points in the set. That is, a state is a pure state if and only if it cannot be expressed as a linear combination of other states in the set, but with the coefficients constrained to the interval [0, 1]. Moreover, a density matrix is a pure state if and only if $\mathrm{Tr}\,\rho^2 = 1$, where Tr means trace.

To illustrate these points, we can use the Peres [19] state again. Let us compare the density matrices and $\mathrm{Tr}\,\rho^2$ for the pure singlet (ρ_{pure}) and ρ_{mixed}.

$$\rho_{\mathrm{pure}} = \begin{bmatrix} 0 & 0 & 0 & 0 \\ 0 & \frac{1}{2} & -\frac{1}{2} & 0 \\ 0 & -\frac{1}{2} & \frac{1}{2} & 0 \\ 0 & 0 & 0 & 0 \end{bmatrix} \tag{4.12}$$

and it is easily computed that $\mathrm{Tr}\,\rho^2_{\mathrm{pure}} = 1$. Whereas, ρ_{mixed}, defined in equation (4.9), gives

$$\mathrm{Tr}\,\rho^2_{\mathrm{mixed}} = \mathrm{Tr} \begin{bmatrix} A & 0 & 0 & 0 \\ 0 & B & C & 0 \\ 0 & C & B & 0 \\ 0 & 0 & 0 & A \end{bmatrix}, \tag{4.13}$$

where

$$A = \frac{(1-x)^2}{16}, \quad B = \frac{(1+x)^2}{16} + \frac{x^2}{4} \quad \text{and} \quad C = \frac{-x-x^2}{4}, \tag{4.14}$$

then $\mathrm{Tr}\,\rho^2_{\mathrm{mixed}} = 2A + 2B \leq 1$, with equality holding only if $x = 1$, that is, the state is a pure singlet state. Notice that when $x = 0$, $\mathrm{Tr}\,\rho^2_{\mathrm{mixed}} = \frac{1}{4}$. In general, a fully mixed state of a density matrix of dimension n has $\mathrm{Tr}\,\rho^2_{\mathrm{mixed}} = 1/n$.

The quantity $\mathrm{Tr}\,\rho^2$ is called the purity of a state because it is a measure of mixedness. We end this section with some explanation of how it works; that is, why $\mathrm{Tr}\,\rho^2 \leq 1$, with equality only when ρ is a pure state. The result is based on Kadison's inequality [21], which states that for a positive and unital map ϕ, then for every Hermitian matrix A

$$\phi(A)^2 \leq \phi(A^2). \tag{4.15}$$

Now, take the map to be $\phi = (1/n)\,\mathrm{Tr}$. A unital map means that it maps the unit to the unit, $\phi(I) = 1$. To ensure this condition for $\mathrm{Tr}\,I_n$, where I_n is the $n \times n$ unit matrix, we need the prefactor $1/n$.

By the spectral theorem, the spectral decomposition of A is given in terms of its n eigenvalues λ_j and the projection operators $P_{\lambda_j} = |v_{\lambda_j}\rangle\langle v_{\lambda_j}|$, where v_j are the eigenvectors of A. Thus [22],

$$A = \lambda_1 P_{\lambda_1} + \cdots + \lambda_n P_{\lambda_n} \tag{4.16}$$

and

$$A^2 = \lambda_1^2 P_{\lambda_1} + \cdots + \lambda_n^2 P_{\lambda_n}, \tag{4.17}$$

where we used the fact that projection operators are idempotent ($P = P^2$). For a finite-dimensional system, we can see that $\lambda_1^2 \leq \lambda_1$, $\lambda_2^2 \leq \lambda_2$ and so on, because each $\lambda_j \leq 1$. So that $\sum \lambda_j^2 \leq \sum \lambda_j = 1$. More generally, it is evident that

$$\phi(A) = \frac{1}{n} \sum \lambda_j \phi(P_{\lambda_j}) \tag{4.18}$$

and

$$\phi(A^2) = \frac{1}{n} \sum \lambda_j^2 \phi(P_{\lambda_j}) \tag{4.19}$$

and for our map $\phi = (1/n)\,\mathrm{Tr}$ with A identified with ρ, we see that $\sum \lambda_j = 1$ by definition of ρ and the limiting cases of $\sum \lambda_j^2$ are $n \times (1/n^2)$ for a fully mixed state and unity for a pure state by the normalization of the wavefunction. Hence

$$\left(\frac{1}{n}\,\mathrm{Tr}\,\rho\right)^2 \leq \frac{1}{n}\,\mathrm{Tr}\,\rho^2 \tag{4.20}$$

because we found that $((1/n)\,\mathrm{Tr}\,\rho)^2 = 1/n$ and $(1/n)\,\mathrm{Tr}\,\rho^2$ can take values in the range $[1/n^2, 1/n]$, where $[\cdots]$ means a closed interval.

Now, because we have just proven that $\mathrm{Tr}\,\rho \leq n\,\mathrm{Tr}\,\rho^2$, and we established that $\mathrm{Tr}\,\rho^2$ can only take values in the interval $[1/n, 1]$, then it follows that

$$\mathrm{Tr}\,\rho^2 \leq \mathrm{Tr}\,\rho = 1. \tag{4.21}$$

A final point to note is that $\mathrm{Tr}\,\rho^2$ is a useful gauge of the mixedness of a state, and because it provides a partial ordering on density matrices, it can compare mixedness. However, it cannot compare the mixedness of density matrices that have different dimension. For example, if we randomly generate molecular aggregates containing different numbers of molecules, we cannot use $\mathrm{Tr}\,\rho^2$ to compare the mixedness of these systems. You can see this immediately by comparing 2×2 and 3×3 fully mixed states, which have $\mathrm{Tr}\,\rho^2$ values of $1/2$ and $1/3$, respectively.

Instead of purity, it is more generally useful to use a measure such as von Neumann entropy, defined with respect to the density matrix for state A as:

$$S(A) = -\,\mathrm{Tr}(\rho_A \log_2 \rho_A). \tag{4.22}$$

Noting that we use logarithm to base 2, then the units of entropy are 'bits'. A pure state has $S = 0$, while a mixed state has a von Neumann entropy less than or equal to the classical (Shannon) entropy. We discuss entropy in [9] and see also [23].

(e) Delocalization versus mixing in molecular excitons

Often we need the entire state space to perform quantum processing, like computing. However, that can be impractical for chemical systems because the states tend to be organized on an energy 'ladder'. For example, double-excitations of molecular excitons are higher in energy than the single-excitation subspace. The main problem is that these higher excitation subspaces are short-lived. If we populate them, say by optical absorption, they decay rapidly to the single-excitation states. Nevertheless, these single-excitation states alone can be a useful resource. Coherent states,

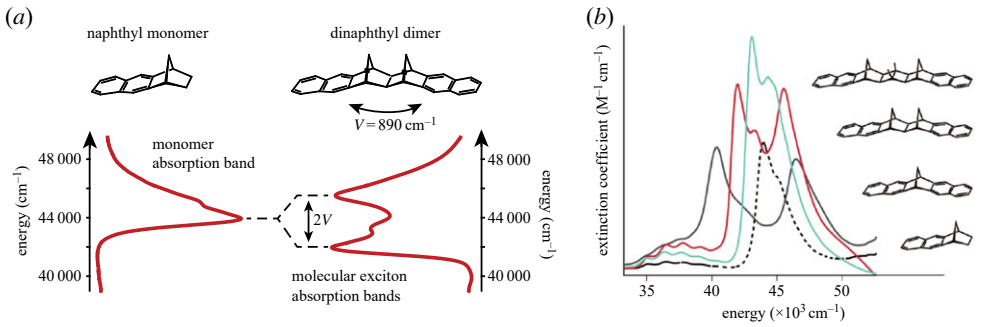

Figure 3. (*a*) The absorption spectrum of a single molecular chromophore in solution (left) compared with a dimer constructed so that the electronic coupling exceeds the line broadening [30]. Note the splitting of the spectral band (by twice the electronic coupling) to form the two excitonic eigenstates. (*b*) Absorption spectra of rigidly linked dinaphthyl molecules DN-2 (black line), DN-4 (red line) and DN-6 (aqua line), where *n* in DN-*n* indicates the number of bonds spanning the norbornane bridge, compared with the model chromophore N-2 (black dotted line). Adapted from Scholes *et al*. [31].

that include excitons, are potentially useful because they provide a resource for allowing quantum operations [23–25].

Molecular excitons are examples of coherent states that have been widely explored in the chemical context. Molecular excitons are collective electronic states that span several molecules [26–28]. The idea is that an excited state molecule couples to a nearby ground state molecule by a resonant interaction between transition densities, often well-approximated as the resonant interaction between transition dipoles [29]. The interaction produces new eigenstates for the electronic excited states of the pair of molecules, as explained in figure 3. The excitonic delocalization produces entangled states in the single-excitation manifold, which in the case of a dimer (two interacting molecules) are the Bell States Ψ_+ and Ψ_-.

Excitonic delocalization is not limited to span only two molecules, but may extend over several molecules, at least, if the electronic coupling is large enough compared with spectral line broadening. The obvious question arises, can we design chemical systems that are more resistant to this decoherence that localizes the state? If so, what are possible design strategies? One obvious way forward is simply to design systems where the molecules interact more strongly. The approach works to some extent, but still allows only relatively short coherence lengths [32].

An idea we explored recently is to exploit emergent states to ensure molecular excitons become more robust to decoherence as they become larger (i.e. comprise more coupled molecules) [16]. The concept is illustrated by some model calculations based on a procedure where we average over site disorder (a distribution of molecular transition energies) in the molecular exciton Hamiltonian to produce density matrices. We calculate the spectrum of the density of excited states by ensemble averaging over the site energy offsets (ϵ_i). To calculate these averages, a form of random matrix theory is used. Random matrix theory for molecular excitons [16,17] is a simple way to calculate ensemble properties of a disordered system.

Examples of calculations produced by the method are shown in figure 4. The properties of various connectivities between absorbing molecules, or sites, are represented by graphs. The nodes of a graph denote the molecules as two-level systems (or qubits), while the edges indicate pairwise electronic couplings. In figure 4*a–c*, we compare three kinds of graphs—nearest neighbour, star, circulant—and graphs comprising 17 or 85 nodes (molecules). The density of excited states are plotted, see Scholes [16] for details. We focus on the state with the lowest eigenvalue, indicated by the arrow.

In the case of nearest neighbour coupling, the von Neumann entropy increases as the number of molecules increases, and the delocalization length of the exciton decreases. Both these factors are consistent with an increase in mixedness of the state for the larger system. The reason for that is the eigenvalues are constrained to lie within the strict bound, relative to zero mean,

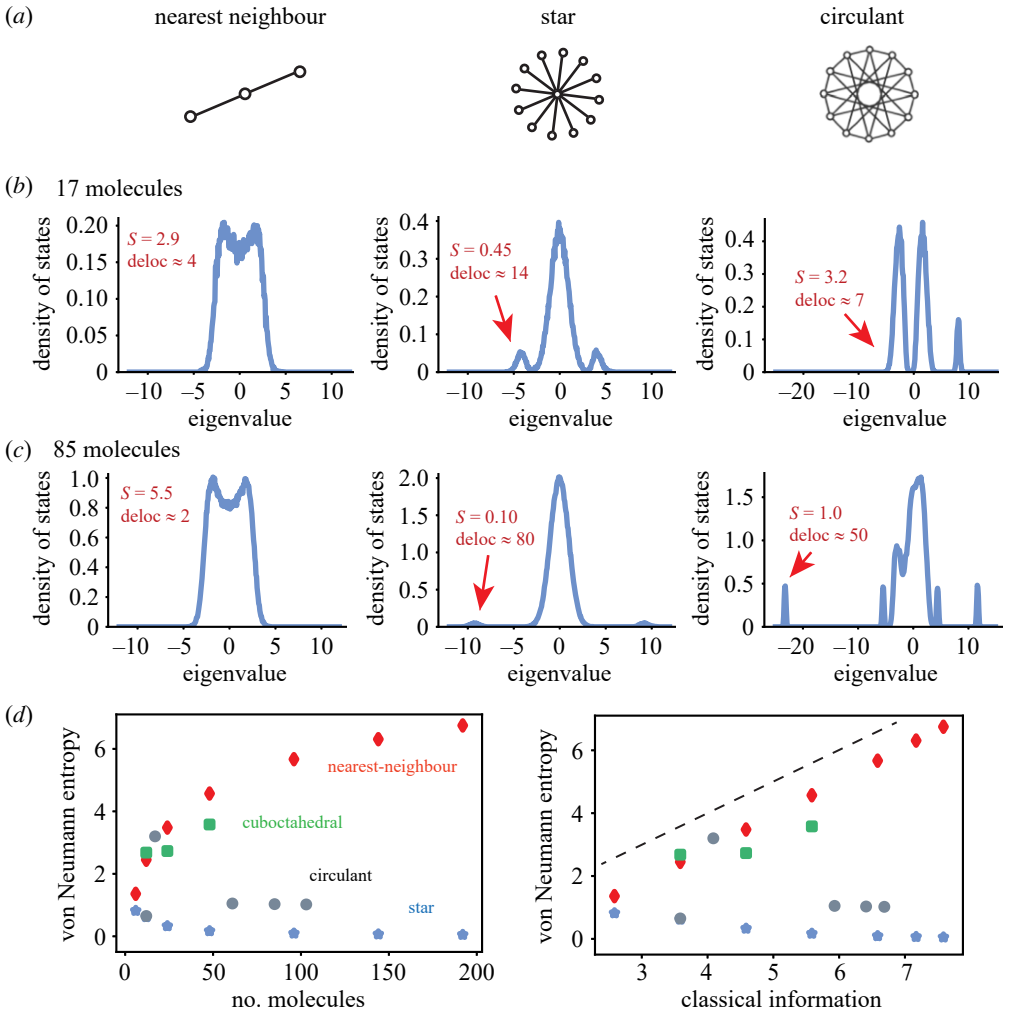

Figure 4. (*a*) Illustrations of the nearest-neighbour, star and circulant graphs. (*b*) Comparison of the density of excited states and coherence metrics for nearest-neighbour, star and circulant graphs for systems containing 17 molecules. (*c*) As for part *b*, but for 85 molecules. (*d*) Predictions of von Neumann entropies for the lowest eigenstates of disordered systems comprising various numbers of molecules. The entropy remains low for the systems that exhibit an emergent state. Adapted from Scholes [16].

$[-2V, 2V]$, where V is the nearest-neighbour electronic coupling. By contrast, notice how the lowest eigenstate in the cases of the star and circulant graphs splits away from the other states, and its separation gets larger when there are more molecules in the system. That state therefore is more resilient to mixing with the other eigenstates, and its mixedness consequently decreases as the system becomes larger.

These remarkable structures show *emergent* properties. That is, at some threshold, an eigenvalue splits always from the main density of states, and that splitting increases as the system size increases. Therefore, counterintuitively, larger systems become more robust. It seems that these kinds of structures should be targets for large systems that retain quantum properties in the lowest eigenstate. Figure 4*d* compares the von Neumann entropy with the classical information expected for a system of various sizes. Notice how some graphs scale with the classical information, these states are strongly mixed. Whereas some graphs, like the circulant and star (among others) stabilize with size. See also that the classical information is a strict upper bound for the quantum information measured by the von Neumann information.

5. A chemical perspective of entanglement

We have seen that the state of an entangled system cannot be decomposed into a product of states assigned to the subsystems, that is, states living exclusively and independently in each qubit's Hilbert space. The form of the superpositions in an entangled state enables new ways to correlate the states of the subsystems, which are not possible for classical systems. The correlations in quantum systems are richer than classical wave superpositions or interferences. A main advantage of the quantum systems is that it takes only a linear amount of classical resources to construct an exponentially large superposition. The way to think about this fact is that in a classical superposition we need to control each bit independently. But for a quantum system, we leverage the tensor product space to provide a set of 'pre-correlated' product states that serve as building blocks from which we can produce the superpositions. We only need to lock the product basis states into some phase relationship, not every qubit within each product state.

Here we aim to provide a few select examples to illustrate how and where quantum information science intersects chemical science. It is not a review, and many other relevant, wonderful examples have been reported that are not included here. The reader is urged to seek them out in the literature. The goal for the present paper is to make a few succinct points using the examples.

(a) Spin eigenstates and singlet fission

A canonical molecular example of states exhibiting quantum correlations is spin eigenstates. In particular, the four spin eigenstates of a two-electron, two-orbital system—the singlet and three triplet states—are equivalent to the four Bell states. Eigenstates comprising more than two-electrons and orbitals provide a rich variety of states that are probably non-separable. The states produced by a process known as 'singlet fission' are a good example of such states. The states relevant for singlet fission have a clear physical attribution, which we describe below to illustrate physically how an entangled state can become approximately separable through mixing [33].

Singlet fission is a process where an initial singlet photoexcitation splits into a four-electron, four-orbital singlet excited state shared across two molecules [34], figure 5*a*. The state thus formed is called the correlated triplet pair. It serves as a good example for how to think about spin correlation that entangles two molecules. The spin eigenfunction of the correlated triplet pair state is given by [33,36,39]

$$|X_1\rangle = \frac{1}{\sqrt{3}}\Big[|\alpha\alpha\beta\beta\rangle + |\beta\beta\alpha\alpha\rangle - \frac{1}{2}\big(|\alpha\beta\alpha\beta\rangle + |\beta\alpha\alpha\beta\rangle + |\alpha\beta\beta\alpha\rangle + |\beta\alpha\beta\alpha\rangle\big)\Big], \tag{5.1}$$

where the 'spin up' and 'spin down' states are indicated as α and β, respectively. Each product is written in a simple form, but it represents the Slater determinant. Note that the key point is we cannot associate any electron to a specific molecule.

The overall entanglement arises physically because the electrons are somewhat delocalized across the molecules (the relevant orbitals overlap) and we cannot distinguish which electrons are associated with which molecule. Our chemical intuition for the correlated triplet pair state is that it comprises two triplet states, one located on each molecule, but with the spins correlated so the overall spin is a singlet. Following this intuitive prescription, if we insist that two electrons are associated with molecule A and the other two electrons with molecule B, then the entanglement across the molecules is destroyed because we can factorize the state into a product of two local states. To show that, let us make the approximation and simplify equation (5.1) by forcing the first two electrons to be associated with molecule A and the second two with molecule B. The state becomes a linear combination of products of local triplet states

$$|X_1\rangle \approx \frac{1}{\sqrt{3}}\Big[|\alpha\alpha\rangle_A|\beta\beta\rangle_B + |\beta\beta\rangle_A|\alpha\alpha\rangle_B - \frac{1}{2}\big(|\alpha\beta\rangle + |\beta\alpha\rangle\big)_A\big(|\alpha\beta\rangle + |\beta\alpha\rangle\big)_B\Big]. \tag{5.2}$$

This association of groups of electrons to specific molecules is a reasonable approximation when the molecules interact weakly and decoherence has localized the state. A formal approach

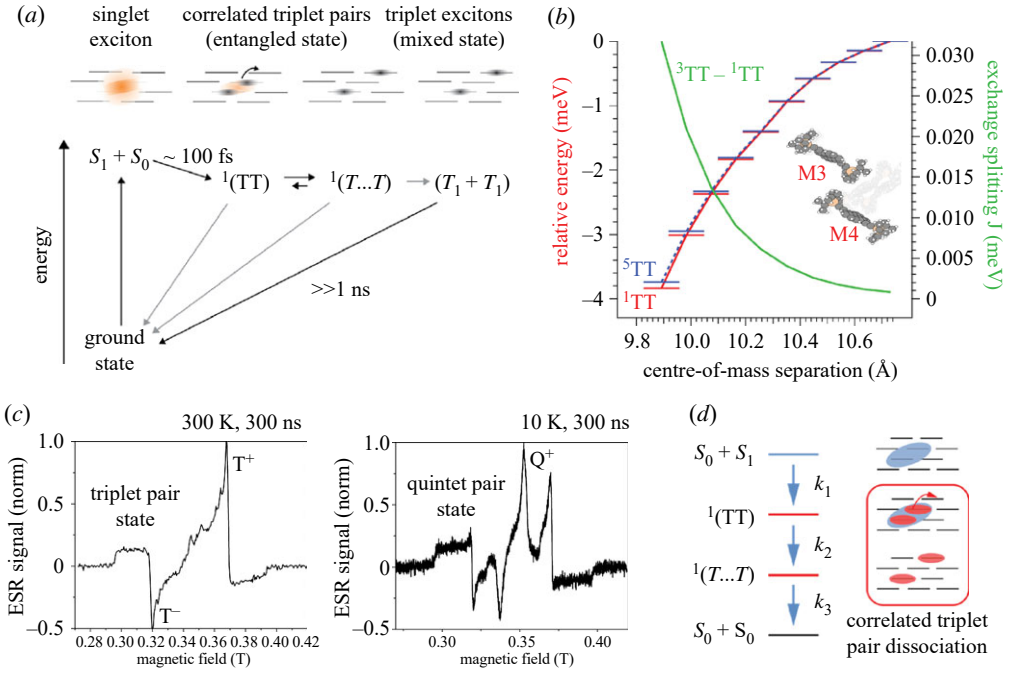

Figure 5. (*a*) Schematic of the different singlet fission intermediates and singlet exciton fission energy level diagram. Adapted with permission from [35]. Copyright 2016 American Chemical Society. (*b*) Energy spacing of the lowest-lying correlated pair levels of TIPS-pentacene dimers estimated using DMRG electronic structure calculations. Adapted with permission from [36] for details. Copyright 2020 American Chemical Society. (*c*) Comparison of time-resolved ESR spectra recorded at 300 K (left) and 10 K (right) of equilibrated correlated pair states in TIPS-tetracene. The new lineshape seen at 10 K is assigned to the quintet correlated pair states. Adapted from [37] based on data at doi:10.17863/CAM.1634. (*d*) Kinetic scheme elucidated from transient absorption spectroscopic studies of TIPS-pentacene films that detected separation of the correlated triplet pair by decay of a spectral signature assigned to the closely separated pair state. Adapted with permission from [38]. Copyright 2018 American Chemical Society.

of electron groups was proposed by McWeeny [40,41], but the relationship of that approximation to loss of quantum correlations spanning the electron groups has not been much explored.

Entanglement across the triplet pair state has been of interest. Researchers have asked how long it lasts, with the answer being many nanoseconds [35,38,42]. The overall-singlet correlated triplet pair is the lowest energy state, but lying close above it in energy are overall-triplet correlated pair states and, above those states, the overall-quintet correlated pair states [36,43,44]. The decoherence mechanism is dominantly population relaxation to these other correlated pair state levels. That equilibration is especially favoured at larger intermolecular separations because the exchange splitting diminishes and all these nine states become closely spaced. Quantum chemical calculations give an estimate of the magnitude of the energy separations between the states [36], figure 5*b*.

Evidence for the equilibration among the states at 300 ns after production of the correlated triplet pair has been ascertained from electron spin resonance (ESR) spectroscopy [37]. For example, figure 5*c* shows that at low temperature the ESR spectrum of the quintet states is comparable in amplitude with that of the triplet correlated pair states [37]. Equilibration among these states produces a mixed state, thereby lessening the entanglement. This is an important observation for quantum information from the chemical perspective: as the separation between molecular subsystems increases, the states become more closely spaced, facilitating thermalization of the population, and thus it becomes difficult to preserve entanglement.

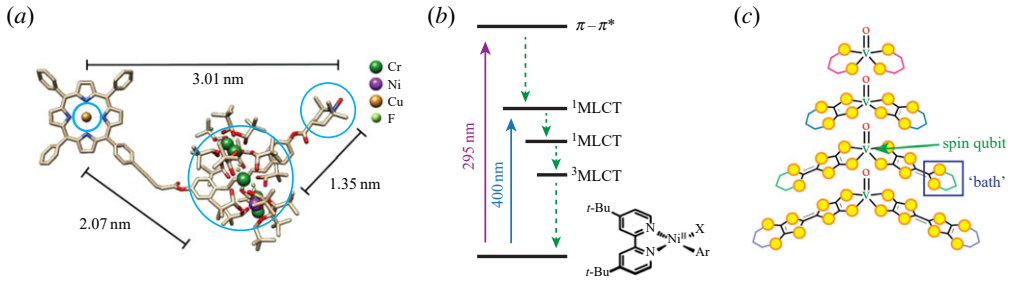

Figure 6. (*a*) Multi-qubit system hosted in a molecular framework. The molecule contains three individually addressable, weakly interacting, spin centres: Cu(II), a Cr_7Ni ring and a nitroxide group, which are circled for clarity. See Rogers *et al*. [56]. Free to read and use from: [56]. Copyright 2022—The Authors. Angewandte Chemie International Edition published by Wiley-VCH GmbH. (*b*) Summary of the electronic excited states and photophysical decay pathways for Ni(II) aryl halide complexes. Adapted with permission from: [64]. Copyright 2018 American Chemical Society. (*c*) Structures of a series of vanadyl complexes used to study electron spin decoherence. The spin qubit is located on the vanadium centre, as indicated. Decoherence is caused, predominantly, by coupling to a 'bath' of spin-active protons positioned at various distances from the qubit. EPR spectroscopy showed how the spin decoherence can be controlled by the distance between the qubit and the spin bath. Adapted with permission from [65]. Copyright 2017 American Chemical Society.

Other questions in the field concern how to detect and exploit the entanglement produced by singlet-fission [33,45–50]. Good evidence that the correlated triplet pair state is entangled across two (or more) molecules is the detection of that totally symmetric double-excitation state in photoluminescence spectroscopy [51] together with the absence of phosphorescence emission from either molecule in the pair.

The separation of the correlated triplet pair state in molecular films has been evidenced in various experiments. It leads to increased distance of entanglement, but it is likely that this also expedites mixing of the state, and loss of entanglement. The manifold of spin states is compressed as the triplet pair becomes more separated, which allows for more effective thermal equilibration and mixing. The correlations ensured by entanglement mean that the population must evolve 'state to state'; the local triplet states do not move independently, and therefore there may be interesting, unexplored, correlations connected with migration of the triplet pair. Experiments have shown that individual triplet states can be 'harvested' from the correlated triplet pair by energy transfer [52], but we do not know whether the harvested triplet excitation remains entangled with its partner. Future work may identify interesting correlations or functions involving the triplet pair state that arise because of entanglement.

(b) Spins in molecules for entanglement

There is good evidence that molecules incorporating unpaired electrons in the ground state, radicals, will serve as interesting resources for quantum processes and qubits [2,53–56]. The teleportation example described earlier is a case in point, showing how spins can be controlled and read out using EPR methods. New work is revealing a fascinating array of stable radical-containing molecules that can be addressed optically [57–63]. In one series of papers [61–63], it has been established that a radical, an unpaired electron serving as a qubit, can interact and entangle with further unpaired spins that are produced upon photoexcitation. The spins exchange-couple with the original spin qubit. In other work [56], a team of researchers synthesized a molecular system serving as a multi-qubit framework. The molecule contains three individually addressable, weakly interacting, spin centres. EPR techniques, again, enable the individual spin qubits to be prepared and measured, figure 6*a*.

Photoswitching and photo-activating radical species can be a useful resource for molecular-scale quantum information systems. However, there are chemical challenges that need further

study. For example, the excited electronic states of radicals have been found to be short-lived, in the range of tens of picoseconds [66,67]. In addition, there are many desirable molecules that incorporate transition metals, where the manifold of excited electronic states is complex and initially photo-excited states relax quickly to lower-lying states, figure 6*b* [64]. An approach for suppressing ultrafast relaxation among excited states is to engineer molecular rigidity into cage-like ligand shells [68].

A topic of importance is how long superposition states involving radical species in chemical systems can survive. Freedman and co-workers designed a series of molecules where a spin qubit is located on a vanadium atom, and a nuclear-spin 'bath' is incorporated in a molecular fragment rich in H atoms that is positioned at various distances from the qubit using spacer 'arms' [65], figure 6*c*. The main result of the work is that when the nuclear spin bath is positioned within a critical radius from the vanadium centre, an abrupt jump in spin coherence time is observed. The results show that within this critical radius, the bath becomes part of the 'system' and no longer exerts a decohering effect.

(c) Charge separation

The separation of charges, an electron and hole, from a photo-excited state has been extensively studied. When the electron and hole remain closely separated, they are said to be 'bound', meaning that they occupy a state—the charge-separated (CS) state. The initial spin eigenstate of the CS state is the same as that of the photo-excited state, often a singlet state and the spins are thus entangled. However, the exchange interaction that splits the singlet and triplet spin manifolds [26] gets markedly smaller as the charges are more separated—because the relevant integral depends on electron-hole overlap. Now, when the singlet and triplet states are closely spaced, the rate of equilibration among the states increases, so the spin state becomes mixed.

A good example of how the mixing of the spin state can be exploited is the concept of a magnetic field sensor, implicated in avian navigation. It is clearly explained by the 'chemical compass' [69]. The principle is to detect properties of a magnetic field through its influence on the singlet-triplet mixing, figure 7*a*. The strategy is to compare the rate of charge separation with the rate of recombination to the initial (singlet) state. At equilibrium, in the absence of mixing, the ratio of rates will obey detailed balance. However, mixing with the triplet states blocks the recombination, thus changing the ratio of rates from that expected by detailed balance. Thus the mixing of the states, which is influenced by an external magnetic field, enables a detector that works based on quantum principles. Interestingly, this example shows that mixing of quantum states is not always a bad thing. The chemical compass described by Maeda *et al*. [69] demonstrates this principle by separating the charges to molecular fragments in a supramolecular triad, depicted in figure 7*a*.

The diminishment of the exchange interaction, and therefore singlet–triplet splitting, with distance, also affects how free charges are generated in organic semiconductors. When the electron and hole separate, but remain close, they collectively comprise the charge transfer state, also termed the charge-transfer exciton, figure 7*b*. A key characteristic of the state is that it can be a pure spin eigenstate, and the spins are entangled. The entanglement goes hand-in-hand with the usual description of the state as comprising a *bound* electron-hole pair. Just like in the example of the chemical compass, the charge-transfer exciton is more likely to recombine to the locally excited state or the ground state when it is a less mixed state.

When the electron and hole are more remote from each other, then their collective state rapidly becomes mixed because the singlet and triplet charge transfer states are very close in energy—the exchange splitting decreases sharply with distance between the electron and hole. When the state is fully mixed, the charge carriers are independent, and they are considered free, or mobile, charges. This provides an interpretation of the established photophysics of charge separation in organic semiconductors [70], but with the additional concept of entanglement among the charge carriers, figure 7*b*. There is a correlation between the concept of electron-hole 'binding' and the

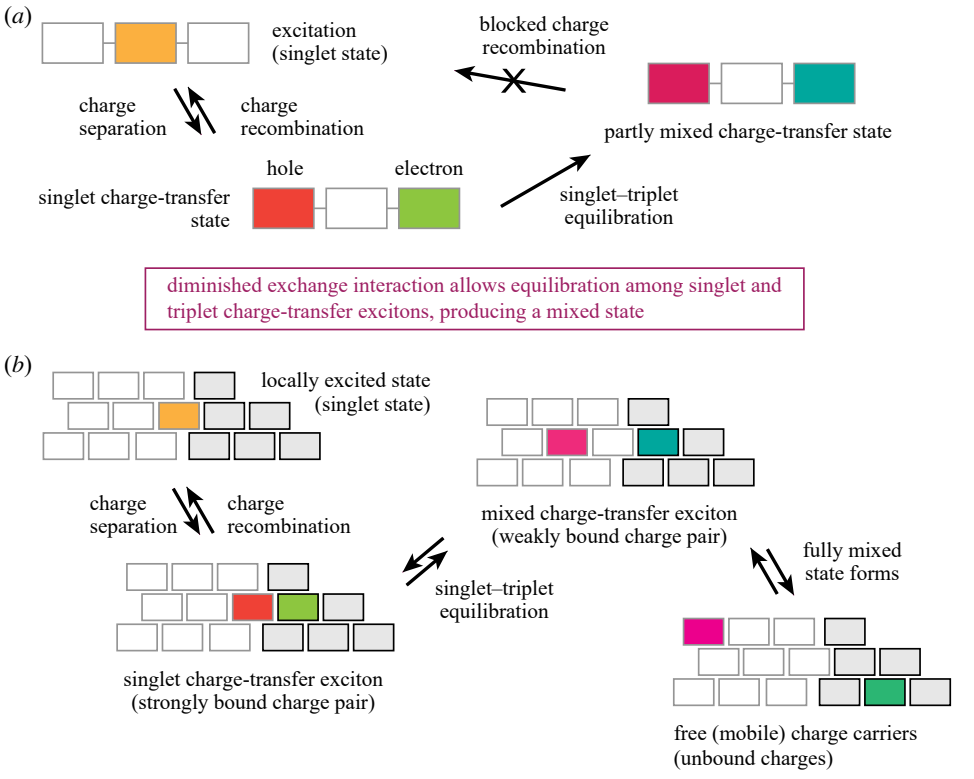

Figure 7. (*a*) Schematic of the reaction scheme that demonstrates the idea of the 'chemical compass' implicated in avian navigation. The supramolecular system comprises three fragments. After the initial charge-separation steps produce a singlet state, a mixed state of the radical pair gradually forms as the population equilibrates among the singlet and triplet states. This, in turn, inhibits back electron transfer. See, for example, Maeda *et al*. [69]. (*b*) A related scheme for the dynamics of charge carrier formation in a donor–acceptor blend of organic semiconductors. The acceptor molecules are shaded grey. This scheme illustrates how mixedness goes hand-in-hand with binding of the electron-hole pair, finally leading to formation of the free charge carriers, that comprise a fully mixed state. See, for example, Rao *et al*. [70] for specific background information.

propensity of the state to be non-separable, which is consistent with the concept of electron groups discussed above. In turn, weakly bound electron-hole pairs comprise a strongly mixed state.

When the electron and hole are unbound, the associated electron groups are distinct, meaning that the electrons are distinguishably associated with one group or the other. That necessarily means that there is no exchange interaction because the Slater determinants are expanded only for the basis functions within each group, then the overall spin eigenstate is a product of spin eigenstates of each group. For example, let us label the electron occupying the highest occupied molecular orbital of molecule A (the electron donor) as a. We label the electrons occupying the highest occupied molecular orbital of molecule B (the electron donor) as b, and the electron in the lowest unoccupied orbital b'. Then the electronic states of the charge-transfer exciton are [71]:

$$^{1,3}\Psi_{CT} = \frac{1}{\sqrt{2}}(|ab\bar{b}'\bar{b}| \mp |\bar{a}bb'\bar{b}|) \tag{5.3}$$

$$^{3}\Psi_{CT} = |abb'\bar{b}| \tag{5.4}$$

and

$$^{3}\Psi_{CT} = |\bar{a}b\bar{b}'\bar{b}|, \tag{5.5}$$

where $|\cdots|$ means Slater determinant. However, for the fully mixed case, the electrons are grouped into two doublet states, one associated with molecule A and one group with B. The

state comprises a statistical mixture of each of the four distinct product states comprising up or down spin of group A and up or down spin of group B. One of these four configurations is

$$\Psi_{CT,\text{mixed}} = \underbrace{|a|}_{\text{group A}}\ \underbrace{|b\bar{b}'\bar{b}|}_{\text{group B}}\ . \tag{5.6}$$

The way that entanglement can be a characteristic of bound carrier pairs and mixedness is a trait of mobile carriers that might be worth exploring further in future work. For example, experiments have shown how a triplet intermolecular radical pair state can be produced in solution, and subsequently the ions have been observed to diffuse apart [72]. Are these separated charge-carrying molecules, in ambient temperature solvent, entangled?

(d) Measuring entanglement

These examples inspire the need to be able to detect entanglement so that the ideas can be tested by experiments. Unfortunately, how to accomplish such measurements on arbitrary quantum states in complex systems remains an open problem. The difficulties are evident by considering how hard it is even to analyse an arbitrary density matrix, which was part of the motivation for going through that process in the preceding sections. A likely way forward will be to devise a witness, or sequence of witnesses, that will allow a subset of quantum correlations in the relevant state space to detected. For an example and pertinent discussion, see Sifain *et al*. [73].

6. Conclusion

We hope that by revisiting some fundamentals of quantum information science, the reader will be inspired to develop new examples where quantum phenomena, such as entanglement, are exploited on the molecular scale. By considering the few chemical examples highlighted in the present paper, it is evident that the immense structural and electronic diversity of molecular systems will be the basis for interesting quantum effects. Molecules can host and organize spins quite precisely on the nanoscale. Many of these systems can also be switched by optical excitation. Excited states can also be readily delocalized across molecules.

Identification of spin eigenstates of molecular systems to entangled states allows connections to be made readily between processes used in quantum information systems, allowing concrete connections between the fields. Establishing these links also helps to reveal challenges facing the application of molecular systems in quantum science. Entanglement can often be robust when the spin eigenstates are well separated in energy, for instance the singlet and triplet states of aromatic organic molecules [26] are separated by energies of the order of 1 eV, and singlet to triplet intersystem crossing happens on the nanosecond timescale. However, as the molecular subsystems become more separated [69], or decoupled [74], the singlet–triplet splitting diminishes, allowing population to equilibrate faster among the spin eigenstates, thus producing a mixed state. This is a factor to consider, and address, when designing protocols where the subsystems are entangled, then separated.

In other words, real systems based on molecules can serve as viable and interesting qubits, but the preservation of entanglement across the molecular subsystems becomes more challenging as the subsystems are separated. At the heart of the matter is the fact that the energy separation between relevant states becomes compressed. That is caused by reduction of the exchange interaction among electrons, which raises the interesting idea that entanglement of electron spins requires the indistinguishability of the electrons. That is, the electron density must overlap across the molecular subsystems.

Data accessibility. The data are all calculated and can be reproduced using the methods described in the paper.

Declaration of AI use. I have not used AI-assisted technologies in creating this article.

Author's contributions. G.S.: conceptualization, funding acquisition, project administration, writing—original draft, writing—review and editing.

Conflict of interest declaration. I declare I have no competing interests.

Funding. This material is based upon work supported by the National Science Foundation (grant no. 2211326) and the Division of Chemical Sciences, Geosciences and Biosciences, Office of Basic Energy Sciences, of the US Department of Energy (grant no. DE-SC0015429).

Acknowledgements. Catrina Oberg, Claire Middlemas and Weijun Wu are thanked for helpful suggestions for improving the paper.

Appendix A. Positive maps and the Peres separability condition

We introduce here a way to identify quantum correlations by examining how a state transforms under positive linear maps. This is a somewhat specialized topic, but gives insight into how entangled quantum states get 'messed up' by certain maps that have no effect on separable states. Thus the topic gives a deeper and potentially more rigorous viewpoint on entanglement from the states perspective—that is, from the properties of the bounded operators on the Hilbert space, the C^*-algebra, rather than the states of the Hilbert space itself. The presentation is only partially rigorous and complete so as to communicate the main, relevant ideas.

We will first establish a little background relevant to the theory of algebra of operators on Hilbert space [75]. To start, note that each element A in the set of linear operators $B(\mathcal{H})$ on the Hilbert space $\mathcal{H}$ can be represented by an $n \times n$ matrix with complex entries. Positivity is an important property of density operators, and ρ therefore is found in the positive cone of $B(\mathcal{H})$. We say that A is positive if [22]

$$\langle x, Ax\rangle \geq 0 \quad \text{for all } x \in \mathcal{H}, \tag{A 1}$$

where the inner product is conjugate linear in the first variable (i.e. the regular physics convention).

There are various conditions for a matrix to be positive, [22] which include:

(i) A is positive if and only if it is Hermitian (that is, $A = A^*$) and all its eigenvalues are non-negative.
(ii) A is positive if and only if $A = B^*B$ for some matrix B.
(iii) A is positive if and only if $A = B^2$ for some matrix B. We write $B = A^{1/2}$.

Now we can define a *positive map*. A linear map $\phi : \mathbb{M}_n \to \mathbb{M}_k$ is said to be a positive map if $\phi(A) \geq 0$ whenever A is positive. Note that $\mathbb{M}_n$ means the set of all $n \times n$ matrices. The map we examined in a previous section, $(1/n)\,\mathrm{Tr}\,A$ is positive (a positive linear functional). The transpose map of A, where the row and column indices are switched, is a positive map. Another positive map used often in quantum mechanics is $\phi(A) = V^*AV$, where V is an $n \times k$ matrix, which maps A from $\mathbb{M}_n$ to $\mathbb{M}_k$.

The matrix units E_{ij} for an $n \times n$ matrix are the set of n matrices where each matrix contains 1 in the i, j entry and zeros everywhere else. There are some examples below. I_m is the $m \times m$ unit matrix (i.e. 1 at each diagonal entry, zeroes elsewhere). $[[E_{ij}]_n]_m$ is the set of $n \times n$ matrix units indexed throughout an $m \times m$ block matrix, with block E_{ij} at entry i, j $(1 \leq m \leq n)$. Similarly, we define $\mathbb{M}_m(\mathbb{M}_n) = \mathbb{M}_m \otimes \mathbb{M}_n$ to be the space of $m \times m$ block matrices $[[A]_n]_m$, whose i, j entry is an element of $\mathbb{M}_n$ (i.e. an $n \times n$ matrix).

Choi worked out a way to characterize maps as positive and completely positive [76]. The main result we need is the way a map on the matrix $\mathbb{M}_m(\mathbb{M}_n)$ can be distributed throughout the matrix by acting on each $\mathbb{M}_n$ block. The map can therefore affect the n part of the tensor product $\mathbb{M}_m \otimes \mathbb{M}_n$ relative to the m part. We will use that property to work out if a state is factorizable with respect to the density matrices of the subsystems (indexed by n and m respectively).

Working through Choi's method provides examples of the introductory points made so far, as well as setting the scene for the remainder of this section. The *Choi matrix* for the map ϕ is

$$C_\phi = \phi \otimes I_p : \mathbb{M}_p(\mathbb{M}_n) \to \mathbb{M}_p(\mathbb{M}_m) = \phi_p([[A]_n]_p) = [[\phi(A)]] \quad \in \quad \mathbb{M}_n \otimes \mathbb{M}_p. \tag{A 2}$$

Choi showed that ϕ is completely positive if and only if C_ϕ is positive for all $1 \leq p \leq m$. That is, we should check that C_ϕ is positive for this entire set of block matrices up to $\mathbb{M}_m(\mathbb{M}_n)$. As we enlarge

the block matrix being considered, we include more of the tensor product structure in the map. In practice, here, we are interested in the simplest example of two interacting qubits, so we only need to consider $p = 1, 2$ to check $\mathbb{M}_2(\mathbb{M}_2)$.

It is easiest to see how this works with a simple example; the transpose map on $\mathbb{M}_2$. The transpose maps of density matrices of our two-level subsystems, ρ_A and ρ_B (elements of $\mathbb{M}_2$), are always positive, which can be demonstrated by considering the 2×2 matrix units:

$$E_{11} = \begin{bmatrix} 1 & 0 \\ 0 & 0 \end{bmatrix}$$

$$E_{12} = \begin{bmatrix} 0 & 1 \\ 0 & 0 \end{bmatrix}$$

$$E_{21} = \begin{bmatrix} 0 & 0 \\ 1 & 0 \end{bmatrix}$$

and

$$E_{22} = \begin{bmatrix} 0 & 0 \\ 0 & 1 \end{bmatrix},$$

which are all positive: the inner product $\langle x, E_{ij}x\rangle = \langle a, a\rangle$, where a means $\alpha|0\rangle$ or $\beta|1\rangle$ and, by definition $\langle a, a\rangle \geq 0$. By the way, hence also $\rho_A \otimes \rho_B$ is positive (see Størmer [77] §6.4).

Now extending to $\mathbb{M}_2(\mathbb{M}_2)$, we write out the full block matrix of units:

$$\begin{bmatrix} E_{11} & E_{12} \\ E_{21} & E_{22} \end{bmatrix} = \left[\begin{array}{cc|cc} 1 & 0 & 0 & 1 \\ 0 & 0 & 0 & 0 \\ \hline 0 & 0 & 0 & 0 \\ 1 & 0 & 0 & 1 \end{array}\right], \tag{A 3}$$

which is Hermitian and has all positive eigenvalues, so it is positive. Then compute C_ϕ with $p = 2$ by evaluating the transpose map,

$$\begin{bmatrix} \phi(E_{11}) & \phi(E_{12}) \\ \phi(E_{21}) & \phi(E_{22}) \end{bmatrix} = \left[\begin{array}{cc|cc} 1 & 0 & 0 & 0 \\ 0 & 0 & 1 & 0 \\ \hline 0 & 1 & 0 & 0 \\ 0 & 0 & 0 & 1 \end{array}\right], \tag{A 4}$$

which has one negative eigenvalue, so the transpose map is not completely positive in this case.

Recalling that our Hilbert space comprising two subsystems is $\mathcal{H} = \mathcal{H}_A \otimes \mathcal{H}_B$, the idea to be demonstrated is that if a state is separable, and therefore factorizable with respect to the density matrices of the subsystems, then any positive map from a state of one subsystem to the other subsystem will be positive. Specifically, Størmer [78], deepening the work of Peres [19] and Horodecki *et al*. [79], proved that a state is separable if and only if

$$C_\phi(\rho) \geq 0 \quad \text{for all normal positive maps } \phi : B(\mathcal{H}_A) \to B(\mathcal{H}_B). \tag{A 5}$$

Here the set of bounded operators on the Hilbert space for subsystem A is $B(\mathcal{H}_A)$, and for subsystem B, $B(\mathcal{H}_B)$. ρ is the density operator corresponding to a state on $B(\mathcal{H}_A) \otimes B(\mathcal{H}_B) = B(\mathcal{H}_A \otimes \mathcal{H}_B)$.

In other words, the state is separable if the Choi matrix is positive for all positive maps on one subspace relative to the other. The density matrix must remain positive, so a map that is not positive tells us that the subsystems are specially correlated—they are entangled. The general difficulty to put this protocol into practice is the 'all'. That is, we might need to check a lot of maps before finding one that is not positive [80–82]. However, Peres [19] showed an example of a map that illustrates the idea well.

The computation of the Peres condition is very similar to the example given above for the transpose map on $\mathbb{M}_2$. Index the density matrix along rows and columns as $|0\rangle_A|0\rangle_B$, $|0\rangle_A|1\rangle_B$, $|1\rangle_A|0\rangle_B$, $|1\rangle_A|1\rangle_B$. Writing $\rho_{mr,ns}$ indicates row indices in the form $|m\rangle_A|r\rangle_B$, and column indices

$|n\rangle_A|s\rangle_B$ for states of the A, B subsystems. Notice that the transpose map yields the matrix $\sigma_{nr,ms}$. Now, for systems comprising a pair of qubits, if σ is positive, then the state is separable, else it is entangled.

To demonstrate, we use the density matrix introduced above that comprises a fraction x or pure singlet Ψ_- and a random fraction $(1-x)$. We put $y=(1-x)/4$ for clarity. We show the partitions of ρ into blocks that delineate the tensor product structure exhibited by a separable state:

$$\rho = \left[\begin{array}{cc|cc} y & 0 & 0 & 0 \\ 0 & y+\frac{x}{2} & -\frac{x}{2} & 0 \\ \hline 0 & -\frac{x}{2} & y+\frac{x}{2} & 0 \\ 0 & 0 & 0 & y \end{array}\right]. \tag{A 6}$$

Then by applying the map $\phi : B(\mathcal{H}_A) \to B(\mathcal{H}_B)$ to each partition of ρ we find

$$\sigma = \left[\begin{array}{cc|cc} y & 0 & 0 & -\frac{x}{2} \\ 0 & y+\frac{x}{2} & 0 & 0 \\ \hline 0 & 0 & y+\frac{x}{2} & 0 \\ -\frac{x}{2} & 0 & 0 & y \end{array}\right]. \tag{A 7}$$

Notice that σ has three eigenvalues of $(1+x)/4$ and one that is $(1-3x)/4$. Hence the state is separable only if $x < \frac{1}{3}$. You can get a physical sense for how this transpose map breaks the entanglement, and is therefore not an allowed map for the quantum state, by seeing how, for example, it switches $|0\rangle_A|1\rangle_B\langle 1|_A\langle 0|_B$ to $|0\rangle_A|0\rangle_B\langle 1|_A\langle 1|_B$.

References

1. Scholes GD *et al.* 2017 Using coherence to enhance function in chemical and biophysical systems. *Nature* **543**, 647–656. (doi:10.1038/nature21425)
2. Wasielewski MR *et al.* 2020 Exploiting chemistry and molecular systems for quantum information science. *Nat. Rev. Chem.* **4**, 490–504. (doi:10.1038/s41570-020-0200-5)
3. Nielsen MA, Chuang IL. 2016 *Quantum computation and quantum information*. Cambridge, UK: Cambridge University Press.
4. Ballentine LE. 2015 *Quantum mechanics: a modern development*. Singapore: World Scientific.
5. Peres A. 1995 *Quantum theory: concepts and methods*. Dordrecht, The Netherlands: Kluwer.
6. Barnett SM. 2009 *Quantum information*. Oxford, UK: Oxford University Press.
7. Horodecki R, Horodecki P, Horodecki M, Horodecki K. 2009 Quantum entanglement. *Rev. Mod. Phys.* **81**, 865–942. (doi:10.1103/RevModPhys.81.865)
8. Vedral V. 2002 The role of relative entropy in quantum information theory. *Rev. Mod. Phys.* **74**, 197–234. (doi:10.1103/RevModPhys.74.197)
9. Wu W, Scholes G. 2023 *Foundations of Quantum Information for Physical Chemistry*. In preparation.
10. Fassioli F, Oblinsky DG, Scholes GD. 2013 Designs for molecular circuits that use electronic coherence. *Faraday Discuss.* **163**, 341–351. (doi:10.1039/c3fd00009e)
11. Chitambar E, Gour G. 2019 Quantum resource theories. *Rev. Mod. Phys.* **91**, 025001. (doi:10.1103/RevModPhys.91.025001)
12. Rugg BK, Krzyaniak MD, Phelan BT, Ratner MA, Young RM, Wasielewski MR. 2019 Photodriven quantum teleportation of an electron spin state in a covalent donor-acceptor-radical system. *Nat. Chem.* **11**, 981–986. (doi:10.1038/s41557-019-0332-8)
13. Holevo A. 2011 *Probabilistic and statistical aspects of quantum theory*. Pisa, Italy: Edizioni della Normale.
14. von Neumann J. 2018 *Mathematical foundations of quantum mechanics*. Princeton, NJ: Princeton University Press.
15. Davies E, Lewis J. 1970 An operational approach to quantum probability. *Commun. Math. Phys.* **17**, 239–260. (doi:10.1007/BF01647093)
16. Scholes GD. 2020 Polaritons and excitons: Hamiltonian design for enhanced coherence. *Proc. R. Soc. A* **476**, 20200278. (doi:10.1098/rspa.2020.0278)
17. Fidder H, Knoester J, Wiersma D. 1991 Optical properties of disordermolecular aggregates:a numerical study. *J. Chem. Phys.* **95**, 7880–7890. (doi:10.1063/1.461317)

18. Vedral V, Plenio M, Rippin M, Knight P. 1997 Quantifying entanglement. *Phys. Rev. Lett.* **78**, 2275–2279. (doi:10.1103/PhysRevLett.78.2275)
19. Peres A. 1996 Separability criterion for density matrices. *Phys. Rev. Lett.* **77**, 1413–1415. (doi:10.1103/PhysRevLett.77.1413)
20. Werner R. 1989 Quantum states with Einstein-Podolsky-Rosen correlations admitting a hidden-variable model. *Phys. Rev. A* **40**, 4277–4281. (doi:10.1103/PhysRevA.40.4277)
21. Kadison R. 1952 A generalized Schwarz inequality and algebraic invariants for operator algebras. *Ann. Math.* **56**, 494–503. (doi:10.2307/1969657)
22. Bhatia R. 2007 *Positive definite matrices*. Princeton, NJ: Princeton University Press.
23. Streltsov A, Adesso G, Plenio MB. 2017 Colloquium: quantum coherence as a resource. *Rev. Mod. Phys.* **89**, 041003. (doi:10.1103/RevModPhys.89.041003)
24. Theurer T, Killoran N, Egloff D, Plenio MB. 2017 Resource theory of superposition. *Phys. Rev. Lett.* **119**, 230401. (doi:10.1103/PhysRevLett.119.230401)
25. Bosyk GM, Losada M, Massri C, Freytes H, Sergioli G. 2021 Generalized coherence vector applied to coherence transformations and quantifiers. *Phys. Rev. A* **103**, 012403. (doi:10.1103/PhysRevA.103.012403)
26. Scholes GD, Rumbles G. 2006 Excitons in nanoscale systems. *Nat. Mater.* **5**, 683–696. (doi:10.1038/nmat1710)
27. Spano FC. 2006 Excitons in conjugated oligomer aggregates, films, and crystals. *Annu. Rev. Phys. Chem.* **57**, 217–243. (doi:10.1146/annurev.physchem.57.032905.104557)
28. Bardeen CJ. 2014 The structure and dynamics of molecular excitons. *Annu. Rev. Phys. Chem.* **65**, 127–148. (doi:10.1146/annurev-physchem-040513-103654)
29. Mirkovic T, Ostroumov EE, Anna JM. 2017 Light absorption and energy transfer in the antenna complexes of photosynthetic organisms. *Chem. Rev.* **117**, 249–293. (doi:10.1021/acs.chemrev.6b00002)
30. Scholes GD, Mirkovic T, Turner DB, Fassioli F, Buchleitner A. 2012 Solar light harvesting by energy transfer: from ecology to coherence. *Energy Environ. Sci.* **5**, 9374–9393. (doi:10.1039/c2ee23013e)
31. Scholes G, Ghiggino K, Oliver A, Paddon-Row M. 1993 Through-space and through-bond effects on exciton interactions in rigidly linked dinaphthyl molecules. *J. Am. Chem. Soc.* **115**, 4345–4349. (doi:10.1021/ja00063a061)
32. Scholes GD. 2020 Limits of exciton delocalization in molecular aggregates. *Faraday Discuss.* **221**, 265–280. (doi:10.1039/C9FD00064J)
33. Scholes GD. 2015 Correlated pair states formed by singlet fission and exciton-exciton annihilation. *J. Phys. Chem. A* **119**, 12 699–12 705. (doi:10.1021/acs.jpca.5b09725)
34. Smith MB, Michl J. 2013 Recent advances in singlet fission. *Annu. Rev. Phys. Chem.* **64**, 361–386. (doi:10.1146/annurev-physchem-040412-110130)
35. Pensack RD *et al.* 2016 Observation of two triplet-pair intermediates in singlet exciton fission. *J. Phys. Chem. Lett.* **7**, 2370–2375. (doi:10.1021/acs.jpclett.6b00947)
36. Taffet EJ, Beljonne D, Scholes GD. 2020 Overlap-driven splitting of triplet pairs in singlet fission. *J. Am. Chem. Soc.* **142**, 20 040–20 047. (doi:10.1021/jacs.0c09276)
37. Weiss LR *et al.* 2017 Strongly exchange-coupled triplet pairs in an organic semiconductor. *Nat. Phys.* **13**, 176–181. (doi:10.1038/nphys3908)
38. Lee TS, Lin YL, Kim H, Pensack RD, Rand BP, Scholes GD. 2018 Triplet energy transfer governs the dissociation of the correlated triplet pair in exothermic singlet fission. *J. Phys. Chem. Lett.* **9**, 4087–4095. (doi:10.1021/acs.jpclett.8b01834)
39. Tao G, Tan Y. 2020 Modular tensor diagram approach for the construction of spin eigenfunctions: the case study of exciton pair states. *J. Phys. Chem. A* **124**, 5435–5443. (doi:10.1021/acs.jpca.0c00263)
40. McWeeny R. 1960 Some recent advances in density matrix theory. *Rev. Mod. Phys.* **32**, 335–369. (doi:10.1103/RevModPhys.32.335)
41. McWeeny R. 1959 The density matrix in many-electron quantum mechanics. 1. Generalized product functions—factorization and physical interpretation of the density matrices. *Proc. Natl Acad. Sci. USA* **253**, 242–259.
42. Pensack RD *et al.* 2018 Striking the right balance of intermolecular coupling for high-efficiency singlet fission. *Chem. Sci.* **9**, 6240–6259. (doi:10.1039/C8SC00293B)
43. Miyata K, Conrad-Burton FS, Geyer FL, Zhu XY. 2019 Triplet pair states in singlet fission. *Chem. Rev.* **119**, 4261–4292. (doi:10.1021/acs.chemrev.8b00572)

44. Casanova D. 2018 Theoretical modeling of singlet fission. *Chem. Rev.* **118**, 7164–7207. (doi:10.1021/acs.chemrev.7b00601)
45. Yong CK *et al.* 2017 The entangled triplet pair state in acene and heteroacene materials. *Nat. Commun.* **8**, 15953. (doi:10.1038/ncomms15953)
46. Matsuda S, Oyama S, Kobori Y. 2020 Electron spin polarization generated by transport of singlet and quintet multiexcitons to spin-correlated triplet pairs during singlet fissions. *Chem. Sci.* **11**, 2934–2942. (doi:10.1039/C9SC04949E)
47. Wan Y, Wiederrecht GP, Schaller RD, Johnson JC, Huang L. 2018 Transport of spin-entangled triplet excitons generated by singlet fission. *J. Phys. Chem. Lett.* **9**, 6731–6738. (doi:10.1021/acs.jpclett.8b02944)
48. Bardeen CJ. 2019 Time dependent correlations of entangled states with nondegenerate branches and possible experimental realization using singlet fission. *J. Chem. Phys.* **151**, 124503. (doi:10.1063/1.5117155)
49. Rugg BK, Smyser KE, Fluegel B, Chang CH, Thorley KJ, Parkin S, Anthony JE, Eaves JD, Johnson JC. 2022 Triplet-pair spin signatures from macroscopically aligned heteroacenes in an oriented single crystal. *Proc. Natl Acad. Sci. USA* **119**, e2201879119. (doi:10.1073/pnas.2201879119)
50. Dill RDD, Smyser KEE, Rugg BKK, Damrauer NHH, Eaves JDD. 2023 Entangled spin-polarized excitons from singlet fission in a rigid dimer. *Nat. Commun.* **14**, 1180. (doi:10.1038/s41467-023-36529-6)
51. Bossanyi DG *et al.* 2021 Emissive spin-0 triplet-pairs are a direct product of triplet-triplet annihilation in pentacene single crystals and anthradithiophene films. *Nat. Chem.* **13**, 163–171. (doi:10.1038/s41557-020-00593-y)
52. He G, Parenti KR, Campos LM, Sfeir MY. 2022 Direct exciton harvesting from a bound triplet pair. *Adv. Mater.* **34**, 2203974. (doi:10.1002/adma.202203974)
53. Troiani F, Affronte M. 2011 Molecular spins for quantum information technologies. *Chem. Soc. Rev.* **40**, 3119–3129. (doi:10.1039/c0cs00158a)
54. Timco GA *et al.* 2009 Engineering the coupling between molecular spin qubits by coordination chemistry. *Nat. Nanotech.* **4**, 173–178. (doi:10.1038/nnano.2008.404)
55. Lavroff RH, Pennington DL, Hua AS, Li BY, Williams JA, Alexandrova AN. 2021 Recent innovations in solid-state and molecular qubits for quantum information applications. *J. Phys. Chem. Lett.* **12**, 10 742–10 745. (doi:10.1021/acs.jpclett.1c03269)
56. Rogers CJ *et al.* 2022 Modelling conformational flexibility in a spectrally addressable molecular multi-qubit model system. *Angew. Chem. Int. Ed. Engl.* **61**, e202207947. (doi:10.1002/anie.202207947)
57. Harvey SM, Wasielewski MR. 2021 Photogenerated spin-correlated radical pairs: from photosynthetic energy transduction to quantum information science. *J. Am. Chem. Soc.* **143**, 15 508–15 529. (doi:10.1021/jacs.1c07706)
58. Yu CJ, von Kugelgen S, Krzyaniak MD, Ji W, Dichtel WR, Wasielewski MR, Freedman DE. 2020 Spin and phonon design in modular arrays of molecular qubits. *Chem. Mater.* **32**, 10 200–10 206. (doi:10.1021/acs.chemmater.0c03718)
59. von Kugelgen S, Krzyaniak MD, Gu M, Puggioni D, Rondinelli JM, Wasielewski MR, Freedman DE. 2021 Spectral addressability in a modular two qubit system. *J. Am. Chem. Soc.* **143**, 8069–8077. (doi:10.1021/jacs.1c02417)
60. Maylander M, Chen S, Lorenzo ER, Wasielewski MR, Richert S. 2021 Exploring photogenerated molecular quartet states as spin qubits and qudits. *J. Am. Chem. Soc.* **143**, 7050–7058.
61. Kirk ML, Shultz DA, Marri AR, Hewitt P, van der Est A. 2022 Single-photon-induced electron spin polarization of two exchange-coupled stable radicals. *J. Am. Chem. Soc.* **144**, 21 005–21 009. (doi:10.1021/jacs.2c09680)
62. Kirk ML, Shultz DA, Hewitt P, van der Est A. 2022 Excited state exchange control of photoinduced electron spin polarization in electronic ground states. *J. Phys. Chem. Lett.* **13**, 872–878. (doi:10.1021/acs.jpclett.1c03491)
63. Kirk ML, Shultz DA, Chen J, Hewitt P, Daley D, Paudel S, van Der Est A. 2021 Metal ion control of photoinduced electron spin polarization in electronic ground states. *J. Am. Chem. Soc.* **143**, 10 519–10 523. (doi:10.1021/jacs.1c04149)
64. Shields BJ, Kudisch B, Scholes GD, Doyle AG. 2018 Long-lived charge-transfer states of nickel(II) aryl halide complexes facilitate bimolecular photoinduced electron transfer. *J. Am. Chem. Soc.* **140**, 3035–3039. (doi:10.1021/jacs.7b13281)

65. Graham MJ, Yu CJ, Krzyaniak MD, Wasielewski MR, Freedman DE. 2017 Synthetic approach to determine the effect of nuclear spin distance on electronic spin decoherence. *J. Am. Chem. Soc.* **139**, 3196–3201. (doi:10.1021/jacs.6b13030)
66. Rieth AJ, Nava M, Nocera DG. 2021 How radical are "radical" photocatalysts? A closed-shell meisenheimer complex is identified as a super-reducing photoreagent. *J. Am. Chem. Soc.* **143**, 14 352–14 359. (doi:10.1021/jacs.1c06844)
67. Baek Y, Reinhold A, Tian L, Jeffrey PD, Scholes GD, Knowles RR. 2023 Singly reduced iridium chromophores: synthesis, characterization, and photochemistry. *J. Am. Chem. Soc.* **145**, 12 499–12 508. (doi:10.1021/jacs.2c13249)
68. Paulus BC, Adelman SL, Jamula LL, McCusker JK. 2020 Leveraging excited-state coherence for synthetic control of ultrafast dynamics. *Nature* **582**, 214–218. (doi:10.1038/s41586-020-2353-2)
69. Maeda K, Henbest KB, Cintolesi F, Kuprov I, Rodgers CT, Liddell PA, Gust D, Timmel CR, Hore PJ. 2008 Chemical compass model of avian magnetoreception. *Nature* **453**, 387–390. (doi:10.1038/nature06834)
70. Rao A, Gillett AJ, Friend RH. 2022 Engineering the spin-exchange interaction in organic semiconductors. *Nat. Mater.* **21**, 976–978. (doi:10.1038/s41563-022-01347-6)
71. Harcourt R, Scholes G, Ghiggino K. 1994 Rate expressions for excitation transfer. 2. Electronic considerations of direct and through-configuration exciton resonance interactions. *J. Chem. Phys.* **101**, 10 521–10 525. (doi:10.1063/1.467869)
72. Vauthey E, Parker V, Nohova B, Phillips D. 1994 Time-resolved resonance raman-study of the rate of separation of a geminate ion-pair into free ions in a medium polarity solvent. *J. Am. Chem. Soc.* **116**, 9182–9186. (doi:10.1021/ja00099a037)
73. Sifain AE, Fassioli F, Scholes GD. 2021 Toward witnessing molecular exciton entanglement from spectroscopy. *Phys. Rev. A* **104**, 042416. (doi:10.1103/PhysRevA.104.042416)
74. Di D *et al.* 2017 High-performance light-emitting diodes based on carbene-metal-amides. *Science* **356**, 159–163. (doi:10.1126/science.aah4345)
75. Takesaki M. 1979 *Theory of operator algebra I*. Encyclopedia of Mathematical Sciences. Berlin, Germany: Springer.
76. Choi M. 1975 Completely positive linear maps on complex matrices. *Linear Alg. Appl.* **10**, 285–290. (doi:10.1016/0024-3795(75)90075-0)
77. Størmer E. 2013 *Positive linear maps of operator algebras*. Heidelberg, Germany: Springer.
78. Størmer E. 2008 Separable states and positive maps. *J. Funct. Anal.* **254**, 2303–2312. (doi:10.1016/j.jfa.2007.12.017)
79. Horodecki M, Horodecki P, Horodecki R. 1996 Separability of mixed states: necessary and sufficient conditions. *Phys. Lett. A* **223**, 1–8. (doi:10.1016/S0375-9601(96)00706-2)
80. Nie J, Zhang X. 2016 Positive maps and separable matrices. *SIAM J. Optim.* **26**, 1236–1256. (doi:10.1137/15M1018514)
81. Bohnet-Waldraff F, Braun D, Giraud O. 2017 Entanglement and the truncated moment problem. *Phys. Rev. A* **96**, 032312. (doi:10.1103/PhysRevA.96.032312)
82. Milazzo N, Braun D, Giraud O. 2020 Truncated moment sequences and a solution to the channel separability problem. *Phys. Rev. A* **102**, 052406. (doi:10.1103/PhysRevA.102.052406)